JACS Au
AN OPEN ACCESS JOURNAL OF THE AMERICAN CHEMICAL SOCIETY

pubs.acs.org/jacsau
Article

α-Synuclein and Mitochondria: Probing the Dynamics of Disordered Membrane-protein Regions Using Solid-State Nuclear Magnetic Resonance

Angelo Gallo,[¶] Silvia Mansueto,[¶] Alessandro Emendato, Giuliana Fusco, and Alfonso De Simone*

Cite This: https://doi.org/10.1021/jacsau.4c00323
Read Online

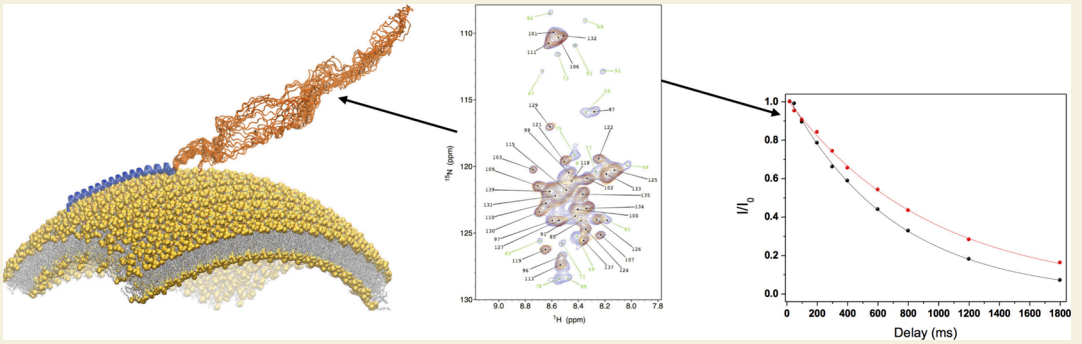

ABSTRACT: The characterization of intrinsically disordered regions (IDRs) in membrane-associated proteins is of crucial importance to elucidate key biochemical processes, including cellular signaling, drug targeting, or the role of post-translational modifications. These protein regions pose significant challenges to powerful analytical techniques of molecular structural investigations. We here applied magic angle spinning solid-state nuclear magnetic resonance to quantitatively probe the structural dynamics of IDRs of membrane-bound α-synuclein (αS), a disordered protein whose aggregation is associated with Parkinson's disease (PD). We focused on the mitochondrial binding of αS, an interaction that has functional and pathological relevance in neuronal cells and that is considered crucial for the underlying mechanisms of PD. Transverse and longitudinal ^{15}N relaxation revealed that the dynamical properties of IDRs of αS bound to the outer mitochondrial membrane (OMM) are different from those of the cytosolic state, thus indicating that regions generally considered not to interact with the membrane are in fact affected by the spatial proximity with the lipid bilayer. Moreover, changes in the composition of OMM that are associated with lipid dyshomeostasis in PD were found to significantly perturb the topology and dynamics of IDRs in the membrane-bound state of αS. Taken together, our data underline the importance of characterizing IDRs in membrane proteins to achieve an accurate understanding of the role that these elusive protein regions play in numerous biochemical processes occurring on cellular surfaces.

KEYWORDS: *α-synuclein, mitochondrial binding, disordered protein regions, membrane-associated proteins, protein dynamics probed by ssNMR*

INTRODUCTION

Proteins embedded or associated with biological membranes generate functionality in living systems, including cellular signaling, drug targeting, the assembly of biomolecular machineries, or the regulation of vesicular trafficking.[1−3] Biophysical and structural methods have achieved an extraordinary resolution in characterizing the detailed molecular properties of homogeneous systems such as transmembrane proteins;[4,5] however, limited success has been obtained in the elucidation of intrinsically disordered regions (IDRs) of proteins bound to lipid bilayers. This gap poses a key challenge in structural biology, as IDRs are often fundamental elements to mediate biological activity and function in protein molecules.[6−11] Molecular simulations represent a precious resource for this research challenge;[12,13] however, inevitable simplifications in the force fields and the reduced accessibility in the size of the systems and time scales of the samplings reduce considerably their applicability. As a result of the limitations in studying protein IDRs in membrane-embedded systems, it is currently challenging to elucidate crucial biochemical mechanisms for the cell. The quantitative characterization of these regions is, however, critical to address

Received: April 11, 2024
Revised: May 13, 2024
Accepted: May 14, 2024

longstanding questions such as for example the transient membrane-protein interactions that regulate synaptic functions and cellular trafficking[14−16] or the action of highly dynamical loops in cell receptors.[17]

Here, we employed solid-state nuclear magnetic resonance (ssNMR) to quantitatively probe the dynamical content of protein IDRs at the surface of lipid bilayers through transverse and longitudinal ^{15}N relaxation. Magic angle spinning (MAS) ssNMR is generally successfully applied to study structurally defined and rigid regions of membrane proteins, typically through cross-polarization (CP) experiments exploiting strong dipolar couplings for the polarization transfer. Recent advances have also enabled the quantification of biomolecular dynamics via CP ssNMR,[18] still in the context of rigid and homogeneous protein states. To quantitatively probe the dynamical content of IDRs of proteins at the surface of biological lipid bilayers, we here measured ^{15}N relaxation through insensitive nuclei enhanced by polarization transfer (INEPT) MAS measurements.[19,20] This method of transferring nuclear spin polarization is largely employed in solution-state NMR and has also been applied in combination with MAS ssNMR to selectively probe the resonances of highly dynamical regions of biomolecules.[20−24] We used INEPT-based MAS ssNMR to quantitatively study the dynamics of the membrane-bound state of α-synuclein (αS), a 14 kDa protein that localizes predominantly at the presynaptic terminals of neurons[25] and whose aberrant aggregation is associated with Parkinson's disease (PD).[8,26−35] We focused on the binding of αS with mitochondria, as evidence exists for the localization of αS on mitochondrial membranes (outer,[36] inner,[37,38] and both types of membranes)[39,40] as well as to mitochondrial-associated membranes.[41] There is large interest in characterizing this interaction owing to the relevance of mitochondrial dysfunction in the pathogenesis of PD and other neurodegenerative disorders.[42−44] Evidences also indicate that αS induces mitochondrial fragmentation[36,45,46] particularly when in the form of the PD variant A53T.[47] Our data elucidate how the spatial proximity with the outer mitochondrial membrane alters the dynamical properties of the disordered C-terminal region of αS compared to its cytosolic state. Taken together, the results of this study underline the importance of characterizing the dynamical properties of IDRs of membrane-associated proteins to study key underlying biochemical mechanisms occurring on cellular and organelle membranes.

RESULTS

Disordered Regions of αS at the Surface of Mitochondrial Membranes

In its functional monomeric state, αS exists in equilibrium between disordered cytosolic and helical membrane-bound states, the latter retaining significant levels of structural disorder.[48,49] This binding is promoted by seven imperfect sequence repeats in the N-terminal region of αS, which encode for amphipathic helical segments.[50−53] Previous MAS ssNMR studies of αS bound to lipid bilayers mimicking synaptic vesicles revealed that the C-terminal region (residues 98−140) has poor membrane association and fully retains its disordered nature,[23,54] the N-terminal region (residues 1−25) folds into a stable amphipathic α-helix at the membrane surface,[55] and the central region (residues 26 to 97) exists in equilibrium between membrane bound (helical) and unbound (disordered) states.[23,56] We here focused on the mitochondrial binding of αS,[57] an interaction that has functional and pathological relevance in neuronal cells.[36−40,58] In particular, using ssNMR ^{15}N relaxation, we quantified the properties of regions of αS retaining significant levels of disorder when bound to the outer mitochondrial membrane (OMM). These membranes differ from other physiological synaptic membranes for which αS binding has been studied,[59,60] as they possess very low cholesterol content (Table 1). In addition to the lipid composition mimicking the physiological OMM, we also considered a mixture containing an excess of cardiolipin (OMM_CL+). The latter is associated with cellular conditions arising as a result of lipid dyshomeostasis in conjunction with neurodegeneration. The excess of cardiolipin in the OMM alters the physicochemical properties of the lipid bilayer, including its charge and fluidity. When estimating the binding affinities of αS to OMM and OMM_CL+, we found stronger interaction for the cardiolipin-rich lipid bilayer (Figure S1), likely due to the higher negative charge. Our structural investigation, however, is independent from the membrane affinity, since ssNMR measurements directly probe the properties of the membrane-bound state of αS regardless of the binding equilibrium.

Table 1. Lipid Molar Fractions in OMM and OMM_CL+

	OMM	OMM_CL+
PC	0.50	0.35
PE	0.28	0.20
PS	0.02	0.014
PI	0.11	0.08
cholesterol	0.09	0.06
CL		0.30

Our goal was to quantify the dynamical content and the conformational properties of IDRs of αS at the surface of mitochondrial-like membranes, including conditions describing the physiological and pathological context. The samples were prepared by incubating acetylated αS (^{15}N labeled) with small unilamellar vesicles (SUV) mimicking the composition of OMM or OMM_CL+. SUVs were prepared via sonication to adopt a diameter distribution of ∼50 nm (Figure S1). This setup maximizes the accessible vesicle surface during the incubation with αS. In order to obtain a comparable amount of membrane-bound αS in the MAS rotors, 30 and 14 mg of protein were incubated with 10 mg of OMM or OMM_CL+ vesicles, respectively, in 20 mM sodium phosphate at pH 6.0 and a total solution volume of 3.5 mL. These incubation conditions counterbalanced the difference in the affinities of αS to bind OMM or OMM_CL+, thereby ensuring that in both experiments 4 mg of protein were pelleted in conjunction with the vesicles via ultracentrifugation. The pellets were then transferred into a 3.2 mm ssNMR zirconia rotor to acquire spectra at a MAS rate of 12.5 kHz. Disordered regions of the membrane-bound αS were probed using ^{1}H-detected HSQC MAS to measure ^{1}H−^{15}N resonances,[20] by acquiring the spectra at a temperature of 25 °C in a data matrix consisting of 1024 (t_2, ^{1}H) × 128 (t_1, ^{15}N) complex points.

MAS ^{1}H−^{15}N HSQC of OMM-bound αS revealed numerous peaks showing a narrow dispersion of the resonances, which is indicative of disordered protein regions (Figure 1A). The detection of these resonances *via* INEPT-NMR indicates that the corresponding residues are poorly associated with the lipid bilayer as they possess very fast local

https://doi.org/10.1021/jacsau.4c00323
JACS Au XXXX, XXX, XXX−XXX

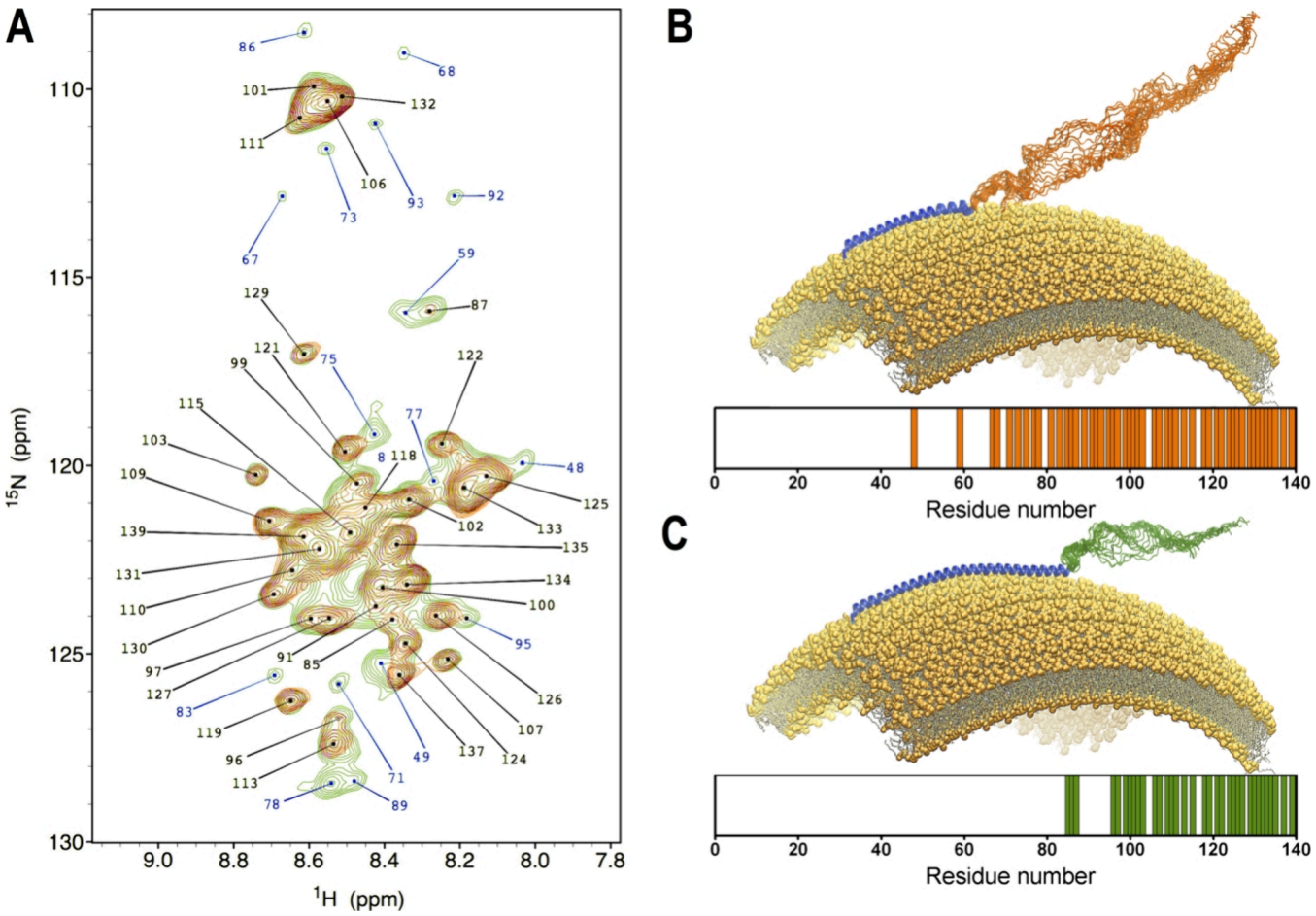

Figure 1. Disordered regions of αS bound to mitochondrial-like membranes probed by ssNMR. (A) ^{1}H-detected ^{1}H−^{15}N-HSQC ssNMR of αS bound to OMM (green spectrum) and OMM_CL+ (red spectrum). Spectra were measured at 25 °C using MAS ssNMR using a 3.2 mm E^{Free} probe with spinning rate of 12.5 kHz, and a ^{1}H Larmor frequency of 700 MHz. The assignment of the spectra was derived by superimposing the ^{1}H−^{15}N-HSQC ssNMR with previously assigned spectra in solution NMR of unbound αS.[54] Residues whose resonances are present only in the OMM-bound spectrum are labeled in blue. Residues whose resonances are present in both spectra are labeled in black. (B, C) Representation of SUV-bound αS. Schematic illustration of the binding mode of αS to OMM (B) and OMM_CL+ (C) vesicles. Bar plots indicate the residues numbers of resonances found in the ^{1}H−^{15}N-HSQC ssNMR of αS-OMM (B) and αS-OMM_CL+ (C). (B) In the case of OMM, numerous residues maintained enough conformational disorder to be detected by ^{1}H−^{15}N-HSQC ssNMR, including a number of residues in the central region. Orange and blue ribbons represent disordered and helical-structured regions of αS bound to OMM. (C) In the case of OMM_CL+ the number of residues that maintain disorder and poor association with the membrane is reduced significantly in the central region. Green and blue ribbons represent disordered and helical-structured regions of αS bound to OMM_CL+.

rotational correlation τ_c. The ^{1}H−^{15}N HSQC ssNMR spectra were indeed found to closely match with those acquired in solution NMR for the cytosolic membrane-unbound αS, thus enabling a convenient assignment of the ssNMR resonances. The αS regions whose resonances appear in the spectra were found to be in part from the C-terminus (residues 98 to 140) and in part from the central region (Figure 1B), including the aggregation-prone nonamyloid β component (NAC) region. More specifically, 58 peaks were detected in the ^{1}H−^{15}N HSQC ssNMR, including 21 that are not part of the C-terminal region (V48, T59, G67, G68, V71, G73, T75, V77, A78, T81, E83, A85, G86, S87, A89, A91, T92, G93, V95, K96, K97). When analyzing the ssNMR spectra of αS bound to OMM_CL+, we found a significant reduction in the number of peaks of the ^{1}H−^{15}N HSQC ssNMR compared to the OMM-bound state (Figure 1A,C). In particular, 34 resonances were observed in this cardiolipin-rich sample, with only five residues (A85, G86, S87, K96, and K97) residing outside the C-terminal region (Figure 1A). Of note, the negatively charged E83 was found to engage more strongly with OMM_CL+, thereby losing dynamical content and falling out the range of detection in INEPT measurements. By contrast, K96 and K97 were found to retain poor association with OMM_CL+ despite being positively charged. This finding indicates that cooperative effects in the αS sequence overwhelm the properties of the individual residues in determining the local dynamical content and membrane interaction.

Taken together, these spectra reveal the topological properties of the membrane-bound state of αS at the surface of mitochondria. Under physiological conditions, αS retains disordered C-terminal and central regions, both showing poor association with the lipid bilayer. Under conditions leading to lipid dyshomeostasis and increase of cardiolipin content in the OMM, the central region of αS mostly disappears from ^{1}H−^{15}N HSQC ssNMR, indicating stronger interaction with the membrane, whereas the C-terminal region remains mostly unbound with the lipid bilayer.

https://doi.org/10.1021/jacsau.4c00323
JACS Au XXXX, XXX, XXX−XXX

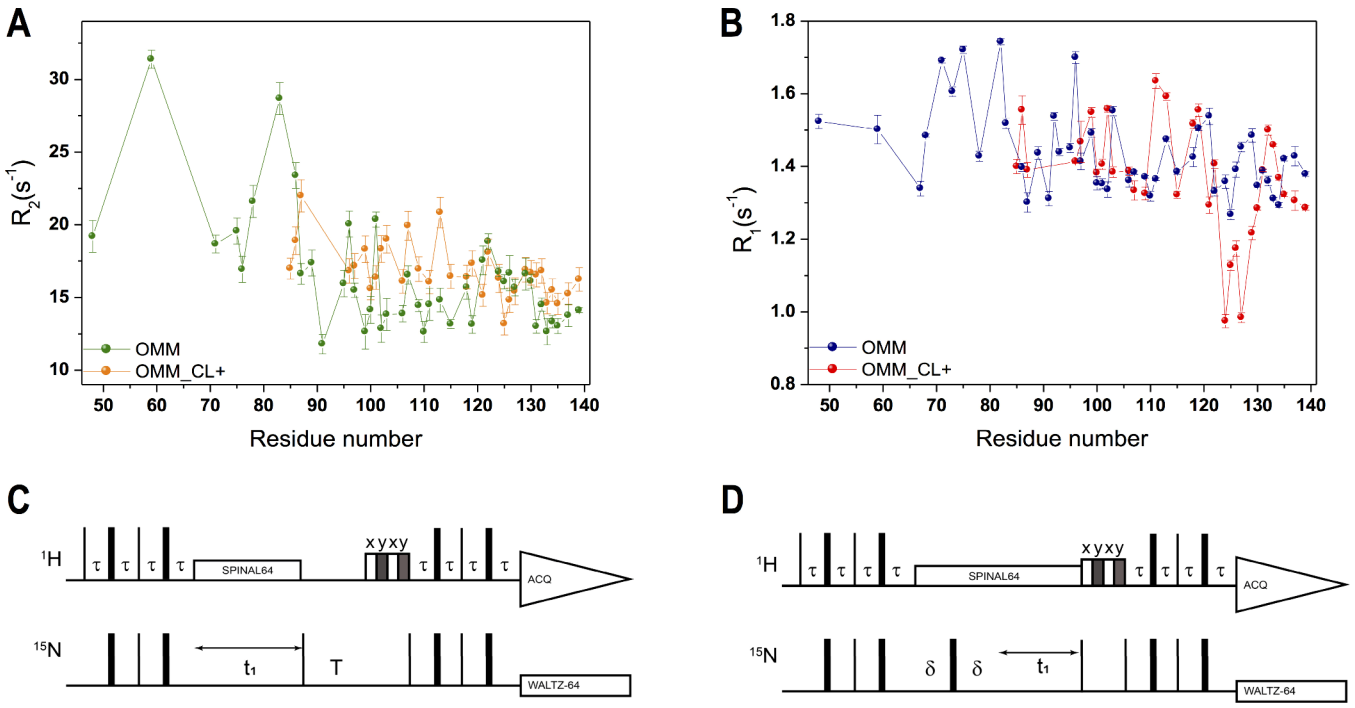

Figure 2. ^{15}N relaxation of disordered regions of αS bound to mitochondrial-like membranes. (A) R_2 values plotted as a function of the αS sequence at the surface of OMM (green) or OMM_CL+ (orange). (B) R_1 values plotted as a function of the αS sequence at the surface of OMM (blue) or OMM_CL+ (red). In panels (A) and (B), we report the value only for residues whose resonances are visible in the INEPT regime, as they remain highly dynamical at the membrane surface. Residues in the N-terminal region are too rigid to be probed with experiments in the INEPT regime. (C) INEPT based ^{1}H−^{15}N HSQC MAS sequence for ^{15}N R_1 relaxation measurements. (D) INEPT based ^{1}H−^{15}N HSQC MAS sequence for ^{15}N R_2 relaxation measurements. Narrow and broad black rectangles represent 90 and 180° hard pulses, respectively. States-TPPI is employed on for the ^{15}N dimension. Evolution time is indicated with t_1. T and δ indicates the relaxation delays for T_1 and T_2 measurements, respectively.

Relaxation Properties of Disordered Regions of αS Bound to Mitochondrial Membranes

We then measured ^{15}N relaxation of membrane-bound αS using INEPT-based MAS ssNMR experiments to probe highly dynamical regions of the protein. Transverse ^{15}N relaxation was acquired in ^{1}H−^{15}N HSQC-based spectra using the MISSISSIPPI water suppression scheme.[61] R_2 values of disordered regions of αS bound to both OMM and OMM_CL+ were found to be generally higher than those of αS in water (Figure 2A and Figure S2A).[60] In particular, αS bound to OMM showed an average R_2 value of 16.5 s^{-1}, which is significantly higher than that observed in the cytosolic state for the same residues (3.9 ± 0.7 s^{-1}, Figure S3). It is likely that the spatial proximity to the membrane surface induced an enhancement in the transverse relaxation, suggesting a weak interaction between the disordered regions of αS and the membrane, in line with previous paramagnetic relaxation experiments with synaptic-like vesicles.[23,54] In a different context, enhancement of a similar magnitude in R_2 values was observed for other disordered proteins when these are studied in crowding conditions,[62] indicating that spatial confinement may be one of the key factors promoting enhanced ^{15}N relaxation. The enhancement in R_2 induced by OMM binding was not homogeneous across the αS sequence, with higher rates observed in the central region (19.8 ± 5.2 s^{-1}) compared to the C-terminal region (14.4 ± 2.0 s^{-1}).

When analyzing the dynamics of disordered regions of αS bound to OMM_CL+, we detected further enhancement of the ^{15}N transverse relaxation (average R_2 values 17.1 ± 1.8 s^{-1}) than the OMM-bound case. This finding indicates that the interaction of disordered regions of αS, including the C-terminus, is stronger with the surface of cardiolipin-rich OMM_CL+, in line with the higher overall binding affinity measured in co-sedimentation essays (Figure S1). The stronger membrane interaction is also consistent with the observation of the broadening of ^{1}H−^{15}N HSQC ssNMR resonances in the central region of αS bound to OMM_CL+ (Figure 1).

When measuring longitudinal ^{15}N relaxation rates (Figure 2B,C), the detected values were found to be in the typical range of other IDPs, indicating that the membrane has no significant effects on R_1 values. In the OMM-bound sample, the average R_1 values were 1.50 ± 0.14 and 1.39 ± 0.07 s^{-1} for the central and C-terminal regions of αS, respectively. Moreover, longitudinal relaxation did not appear to be influenced by cardiolipin, as the αS-OMM_CL+ measurement resulted in R_1 values similar to those of the corresponding regions in the αS-OMM sample (average value of 1.37 ± 0.16 s^{-1}). Some residues of αS, however, showed peculiar R_1 rates in the OMM_CL+ sample with respect to the reminder of the protein. In particular, in the region 124-AYEMPS-129, which is flanked by three negatively charged amino acids (E123, E130, and E131), we detected a significant reduction in the R_1 values (average value of 1.09 ± 0.11 s^{-1}). This observation suggests that the membrane enrichment in cardiolipin content influences the conformational dynamics of the region 124−129 of αS, presumably for a charge effect. It is likely that alterations of the local charge in the αS sequence, e.g., by phosphorylation of S129[63] or by Ca^{2+} binding,[64] are also able to modulate the conformational properties of αS at

https://doi.org/10.1021/jacsau.4c00323
JACS Au XXXX, XXX, XXX−XXX

mitochondrial surfaces thereby influencing its behavior in function and aggregation. Taken together, these relaxation data indicate that disordered regions in the bound state of αS possess unique dynamical properties that, as a result of the membrane proximity, diverge from the corresponding regions in the cytosol. When probing disordered regions in the membrane-bound state of αS, relaxation measurements in solution NMR did not detect significant differences in the OMM and OMM_CL+ samples (Figure S3). Enhanced transverse relaxation was indeed only observed for the N-terminal and central region of αS in the case of OMM_CL+, whereas R_2 values of the C-terminal region and R_1 values of the entire protein showed no difference in the two samples and with respect to the isolated protein case. This finding supports the present MAS ssNMR approach as a powerful direct probe of disordered protein regions at the membrane surface.

DISCUSSION

The characterization of the structural dynamics of backbone and side chains of protein molecules is of fundamental importance to delineate how their biological activity is attained under functional and pathological conditions. Highly dynamical protein regions are often involved in crucial mechanisms such as cell signaling, the response to ligand binding, and conformational switches via post-translational modifications. It is also now established that IDRs of membrane proteins play key roles in molecular interactions that govern fundamental biochemical processes at the surface of the cell and its organelles.[65−68] Characterizing these disordered protein regions when bound with lipid bilayers is therefore a crucial challenge in biochemistry but one that cannot be tackled using some of the powerful techniques of structural biology such as X-ray crystallography and cryo-EM, which are primarily tailored to probe homogeneous and rigid protein states.

A number of experiments exist in solution-state NMR to investigate the dynamical properties of protein IDRs,[9,62,69−71] many of which based on nuclear spin relaxation. When studying membrane proteins, however, solution NMR requires the solubilization via detergent micelles, bicelles, or nanodiscs,[72] but the physiological relevance of these assemblies might be limited. In this context, solid-state NMR (ssNMR) has emerged as a powerful analytical method to study proteins embedded in their native membrane environment, thereby ensuring the functional-structural integrity of the molecule under physiological conditions.[73−75] As most of the ssNMR methods are based on cross-polarization (CP) transfer, their applicability remains primarily tailored to rigid moieties of proteins, with poor sensitivity achieved in the case of IDRs. The long T_2 relaxation of highly mobile residues, however, enables to probe these regions *via* through-bond INEPT coupled with MAS ssNMR.[20,76−80] We here exploited INEPT-ssNMR to probe the conformational properties of disordered regions of αS bound to OMM and OMM_CL+. The interaction with lipid bilayers is a key element for the biological properties of αS, as most of its putative functions are exerted in the membrane-bound state.[25] In its cytosolic state, αS is fully disordered,[50,70,81] whereas upon membrane binding, it partially folds into a helical-rich conformation[48,49] while retaining significant levels of conformational disorder. IDRs in the membrane-bound state of αS include primarily the C-terminal region (residues 98−140), and have been shown to mediate key protein−protein interactions[82] as well as calcium binding[64] within the regulation of the trafficking of synaptic vesicles. Studying the properties of these regions at the membrane surface is therefore a critical goal to elucidate how the balance between function and aggregation is regulated for αS.

We here showed the importance of quantitatively probing the dynamical nature of IDRs in proteins associated with lipid bilayers by focusing on the properties of αS bound to the outer mitochondrial membrane (OMM). Our data show that binding to OMM generates a peculiar structural topology of αS where the C-terminal region, and a significant portion of the central region that includes residues of the NAC remain disordered and poorly associated with the lipid bilayer. This topology may have significant relevance for the promotion of membrane-membrane interactions by αS through the double anchor mechanism,[23] which requires simultaneous binding across two different membranes of the N-terminal and central regions of the protein. The detected exposure of amyloidogenic sequences in the central region of αS might also have relevance in the context of aberrant aggregation at the OMM surface in the context of mitochondrial dysfunction and/or dysregulation.

Under pathological conditions leading to lipid dyshomeostasis, OMM has been shown to accumulate anomalous high levels of cardiolipin,[83] which modify both the fluidity and charge of the lipid bilayer. Our data show that, in the presence of cardiolipin, the αS binding to OMM is altered leading to a loss of dynamics in the central region, which is mostly no longer detectable in INEPT-ssNMR, as well as to changes in the relaxation properties of the segment 124-AYEMPS-129, likely due to charge alteration of the membrane. In addition, our INEPT-ssNMR relaxation data showed that IDRs of αS possess significantly higher R_2 values at the membrane surface compared to the cytosolic state, thus providing evidence of a degree of interaction between these regions and the lipid bilayer. Further enhancement of the transverse relaxation in IDRs of αS was found in the case of binding to cardiolipin-rich OMM, suggesting a stronger local interaction with this lipid mixture.

In summary, the ssNMR spectra and relaxation data presented in this work underline the importance of studying the conformational properties of IDRs at the membrane surface. The properties of these IDRs appear to be significantly different from those of purely random coil states and to be strongly influenced by the properties of the lipid bilayer. Considering the fundamental relevance of IDRs in membrane-associated proteins, the present study defines a key challenge for structural biology to delineate how these regions can be regulated in functional and pathological contexts.

MATERIAL AND METHODS

αS Expression and Purification

αS was expressed and purified in *E. coli* using plasmid pT7−7 as previously described.[54] In order to obtain N-terminal acetylation of αS, we coexpressed this plasmid with one carrying the components of the NatB complex (Addgene). After transforming in BL21 (DE3)-gold cells (Agilent Technologies, Santa Clara, USA), uniformly ^{15}N-labeled αS variants were obtained by growing the bacteria in isotope-enriched M9 minimal media containing 1 g·L^{-1} of ^{15}N ammonium chloride, 2 g·L^{-1} of ^{12}C-glucose (Sigma-Aldrich, St Louis, USA), and 1 g of protonated IsoGro ^{15}N (Sigma, St. Louis, MO). The growth was obtained at 37 °C under constant shaking at 250 rpm and supplemented with 100 μg·mL^{-1} ampicillin and 12.5 μg mL^{-1} chloramphenicol to an OD600 of 0.6. The expression was induced

https://doi.org/10.1021/jacsau.4c00323
JACS Au XXXX, XXX, XXX−XXX

with 1 mM isopropyl β-D-1-thiogalactopyranoside (IPTG) at 37 °C for 4 h, and the cells were harvested by centrifugation at 6200*g* (Beckman Coulter, Brea, USA). The cell pellets were resuspended in lysis buffer (10 mM Tris-HCl pH 8, 1 mM EDTA and EDTA-free complete protease inhibitor cocktail tablets obtained from Roche, Basel, Switzerland) and lysed by sonication. The cell lysate was centrifuged at 22,000*g* for 30 min to remove cell debris. In order to precipitate the heat-sensitive proteins, the supernatant was then heated for 20 min at 70 °C and centrifuged at 22,000*g*. Subsequently, streptomycin sulfate was added to the supernatant to a final concentration of 10 mg·mL^{-1} to stimulate DNA precipitation. The mixture was stirred for 15 min at 4 °C followed by centrifugation at 22,000*g*. Then, ammonium sulfate was added to the supernatant to a concentration of 360 mg·mL^{-1} in order to precipitate the protein. The solution was stirred for 30 min at 4 °C and centrifuged again at 22,000*g*. The resulting pellet was resuspended in 25 mM Tris-HCl, pH 7.7, and dialyzed against the same buffer in order to remove salts. The dialyzed solutions were then loaded onto an anion exchange column (26/10 Q sepharose high performance, GE Healthcare, Little Chalfont, UK), eluted with a 0−1 M NaCl step gradient, and then further purified by loading onto a size exclusion column (Hiload 26/60 Superdex 75 preparation grade, GE Healthcare, Little Chalfont, UK). All the fractions containing the monomeric protein were pooled together and concentrated by using Vivaspin filter devices (Sartorius Stedim Biotech, Gottingen, Germany). The purity of the aliquots after each step was analyzed by SDS-PAGE, and the protein concentration was determined from the absorbance at 275 nm using an extinction coefficient of 5600 M^{-1} cm^{-1}.

SUV Preparation

SUVs were prepared using lipids from Avanti Polar Lipids Inc. (Alabaster, USA) or Sigma-Aldrich (St Louis, USA), and mixed in chloroform solutions.[23,60] The OMM mixture was composed of POPC (1-palmitoyl-2-oleoyl-glycero-3-phosphocholine; Avanti code: 850457C), POPE (1-palmitoyl-2-oleoyl-sn-glycero-3-phosphoethanolamine; Avanti code: 850757C), POPS (1-palmitoyl-2-oleoyl-sn-glycero-3-phospho-L-serine; Avanti code: 840034C), PI (L-α-phosphatidylinositol; Avanti code: 840042C), and cholesterol (Sigma code: C8667) in a molar ratio of 0.5:0.28:0.02:0.11:0.09. OMM_CL+ were prepared with 30% of cardiolipin (CL; Avanti code: 840012C) using a molar ratio of 0.35:0.2:0.014:0.08:0.06:0.3 for POPC:POPE:POPS:PI:cholesterol:CL (Table 1). The lipid mixture in chloroform solution was evaporated under a stream of nitrogen gas and then dried under vacuum to yield a lipid thin film. The thin film was rehydrated by adding aqueous buffer (20 mM sodium phosphate pH 6.0) at a final concentration of 10 mg mL^{-1} and sonicated in an ultrasonic bath for 2 min. SUVs were obtained by using 5 cycles of freeze−thawing and then sonication with an ultrasonic homogenizer until clearance of the mixture. The average diameter of the pore is around 50 nm as controlled using dynamic light scattering (DLS) (Figure S1A).

Magic Angle Spinning (MAS) Measurements

MAS ssNMR measurements were used to directly probe the resonances of αS in the vesicle-bound state, which are inaccessible to solution-state NMR. MAS experiments were carried out on a 700 MHz Bruker spectrometer with a 3.2 mm E^{Free} probe. Insensitive nuclei enhanced by polarization transfer (INEPT) spectra[19] were measured at 25 °C using an MAS rate of 12.5 kHz. ^{1}H detected ^{1}H−^{15}N-HSQC ssNMR of membrane bound αS was measured as in Gopinath et al.[20] Assignments of the resonances of αS in ^{1}H−^{15}N-HSQC ssNMR were derived by superimposing the ssNMR spectra with solution NMR spectra of membrane-free protein using our previous assignments of cytosolic αS.[54]

Transverse and Longitudinal Relaxation Measurements in MAS ssNMR

^{15}N relaxation in the INEPT regime was measured using the pulse sequences shown in Figure 2C,2D. The value of τ was 2.63 ms. ^{1}H SPINAL decoupling with a rf-field strength of 5 kHz was applied during the relaxation delays followed by MISSISSIPPI water suppression scheme.[61] ^{15}N WALTZ decoupling with a rf-field strength of 15 kHz was used during the acquisition time. Both longitudinal and transverse relaxation were acquired with an interleaved scheme. Longitudinal ^{15}N relaxation was measured in ^{1}H−^{15}N HSQC-based ssNMR spectra, using delay times of 20, 50, 100, 200, 300, 400, 600, 800, 1200, and 1800 ms. Transverse ^{15}N relaxation was measured in ^{1}H−^{15}N HSQC-based ssNMR spectra, using delay times of 1, 5, 10, 20, 30, 40, 50, 60, 80, and 120 ms.

Transverse and Longitudinal Relaxation Measurements in Solution NMR

^{15}N transverse and longitudinal relaxation of αS incubated with OMM and OMM_CL+ were measured with standard BRUKER pulse sequences in solution NMR,[84] including the watergate sequence[85] to improve water suppression. R_1 and R_2 values were obtained by fitting the experimental data with single exponential decays; the fitting of experimental data and the error analyses were performed with the program SPARKY. ^{15}N relaxation was measured at 10 °C on a sample composed of αS (300 μM) incubated with the two types of SUVs at a concentration of 0.6 mg/mL and using a BRUKER spectrometer operating at ^{1}H Larmor frequency of 700 MHz equipped with triple resonance HCN cryo-probe. Assignment of the solution NMR resonances was obtained from our previous studies[86] and verified by a series of 3D spectra by following a previously published protocol.[87]

αS-Membrane Binding Affinity from Co-sedimentation Assay

The co-sedimentation assay was employed to estimate the fraction of membrane bound and unbound states as a function of the vesicle concentration. αS and SUVs were both dialyzed in 20 mM sodium phosphate buffer at pH 6.0. The samples were prepared in a total volume of 250 μL, with an array of conditions where the concentration of the protein was kept constant at 50 μM, whereas SUVs had concentrations ranging from 0 to 8 mM. The samples were incubated at room temperature for 1 h and then ultracentrifuged at 361,000*g* for 1 h (Optima Max-XP Ultracentrifuge, Beckman Coulter) using an MLA-150 fixed angle rotor. The concentration of the protein in the supernatant was then used to estimate the fraction of bound protein in each well. This was determined using the Bradford assay by measuring the absorbance at 595 nm and then plotting the data in a BSA standard curve.

We used the Hill equation to fit the co-sedimentation assay titrations (Figure S1B) and calculated an apparent dissociation constant, K_D:

$$\chi_B = \frac{[\text{Lipid}]^n}{K_D + [\text{Lipid}]^n}$$

where χ_B is the fraction of bound protein, K_D is the apparent dissociation constant, and n is the Hill coefficient describing the cooperativity of the process. The resulting apparent K_D values were 4.5 ± 0.3 and 0.9 ± 0.5 for OMM and OMM_CL+, respectively. The Hill coefficients were 2.1 ± 0.6 and 0.4 ± 0.1 for OMM and OMM_CL+, respectively.

Dynamic Light Scattering (DLS)

DLS measurements of vesicle size distributions were performed using a Zetasizer Nano ZSP instrument (Malvern Instruments, Malvern, UK) with backscatter detection at a scattering angle of 173°. The viscosity (0.8882 cP) and the refractive index (1.330) of water were used as parameters for the buffer solution, and the material properties of the analyte were set to those of the lipids (absorption coefficient of 0.001 and refractive index of 1.440). SUVs were used at a concentration of 0.1% in these measurements and the experiments were performed at 25 °C. The acquisition time for the collection of each data set was 5 s, and accumulation of the correlation curves was obtained using 10 repetitions. Each measurement was repeated 3 times to estimate standard deviations and average values of the centers of the size distributions.

https://doi.org/10.1021/jacsau.4c00323
JACS Au XXXX, XXX, XXX−XXX

■ ASSOCIATED CONTENT

Supporting Information

The Supporting Information is available free of charge at https://pubs.acs.org/doi/10.1021/jacsau.4c00323.

Dynamic light scattering of the size of the vesicles; binding curves from co-sedimentation essays; and ^{15}N transverse relaxation probed with MAS ssNMR and solution NMR (PDF)

■ AUTHOR INFORMATION

Corresponding Author

Alfonso De Simone − *Department of Pharmacy, University of Naples, Naples 80131, Italy; Department of Life Sciences, Imperial College London, London SW7 2AZ, U.K.;* orcid.org/0000-0001-8789-9546; Email: alfonso.desimone@unina.it

Authors

Angelo Gallo − *Department of Chemistry, University of Turin, Turin 10124, Italy;* orcid.org/0000-0001-9778-4822

Silvia Mansueto − *Department of Pharmacy, University of Naples, Naples 80131, Italy;* orcid.org/0009-0001-9675-7096

Alessandro Emendato − *Department of Pharmacy, University of Naples, Naples 80131, Italy*

Giuliana Fusco − *Department of Pharmacy, University of Naples, Naples 80131, Italy; Centre for Misfolding Diseases, Department of Chemistry, University of Cambridge, Cambridge CB2 1EW, U.K.;* orcid.org/0000-0002-3644-9809

Complete contact information is available at: https://pubs.acs.org/10.1021/jacsau.4c00323

Author Contributions

¶A.G. and S.M. contributed equally to the present work.

Notes

The authors declare no competing financial interest.

■ ACKNOWLEDGMENTS

This research was supported by the European Research Council (ERC -BioDisOrder -819644 to A.D.).

■ REFERENCES

(1) Munro, S. Lipid rafts: elusive or illusive? *Cell* **2003**, *115* (4), 377−88.

(2) Hernandez, J. M.; Stein, A.; Behrmann, E.; Riedel, D.; Cypionka, A.; Farsi, Z.; Walla, P. J.; Raunser, S.; Jahn, R. Membrane fusion intermediates via directional and full assembly of the SNARE complex. *Science* **2012**, *336* (6088), 1581−4.

(3) Jahn, R.; Lang, T.; Sudhof, T. C. Membrane fusion. *Cell* **2003**, *112* (4), 519−33.

(4) Chandonia, J. M.; Brenner, S. E. The impact of structural genomics: expectations and outcomes. *Science* **2006**, *311* (5759), 347−51.

(5) Fernandez-Leiro, R.; Scheres, S. H. Unravelling biological macromolecules with cryo-electron microscopy. *Nature* **2016**, *537* (7620), 339−46.

(6) Latorraca, N. R.; Venkatakrishnan, A. J.; Dror, R. O. GPCR Dynamics: Structures in Motion. *Chem. Rev.* **2017**, *117* (1), 139−55.

(7) Zhou, M.; Robinson, C. V. Flexible membrane proteins: functional dynamics captured by mass spectrometry. *Curr. Opin Struct Biol.* **2014**, *28*, 122−30.

(8) Fusco, G.; Chen, S. W.; Williamson, P. T. F.; Cascella, R.; Perni, M.; Jarvis, J. A.; Cecchi, C.; Vendruscolo, M.; Chiti, F.; Cremades, N.; et al. Structural basis of membrane disruption and cellular toxicity by alpha-synuclein oligomers. *Science* **2017**, *358* (6369), 1440−3.

(9) Bah, A.; Vernon, R. M.; Siddiqui, Z.; Krzeminski, M.; Muhandiram, R.; Zhao, C.; Sonenberg, N.; Kay, L. E.; Forman-Kay, J. D. Folding of an intrinsically disordered protein by phosphorylation as a regulatory switch. *Nature* **2015**, *519* (7541), 106−9.

(10) Gustavsson, M.; Verardi, R.; Mullen, D. G.; Mote, K. R.; Traaseth, N. J.; Gopinath, T.; Veglia, G. Allosteric regulation of SERCA by phosphorylation-mediated conformational shift of phospholamban. *Proc. Natl. Acad. Sci. U. S. A.* **2013**, *110* (43), 17338−43.

(11) Toyama, Y.; Harkness, R. W.; Kay, L. E. Structural basis of protein substrate processing by human mitochondrial high-temperature requirement A2 protease. *Proc. Natl. Acad. Sci. U. S. A.* **2022**, *119* (17), e2203172119.

(12) Cournia, Z.; Allen, T. W.; Andricioaei, I.; Antonny, B.; Baum, D.; Brannigan, G.; Buchete, N. V.; Deckman, J. T.; Delemotte, L.; Del Val, C.; et al. Membrane Protein Structure, Function, and Dynamics: a Perspective from Experiments and Theory. *J. Membr. Biol.* **2015**, *248* (4), 611−40.

(13) Karplus, M.; McCammon, J. A. Molecular dynamics simulations of biomolecules. *Nat. Struct. Biol.* **2002**, *9* (9), 646−52.

(14) Baker, R. W.; Jeffrey, P. D.; Zick, M.; Phillips, B. P.; Wickner, W. T.; Hughson, F. M. A direct role for the Sec1/Munc18-family protein Vps33 as a template for SNARE assembly. *Science* **2015**, *349* (6252), 1111−4.

(15) Rizo, J.; Xu, J. The Synaptic Vesicle Release Machinery. *Annu. Rev. Biophys* **2015**, *44*, 339−67.

(16) Alabi, A. A.; Tsien, R. W. Perspectives on kiss-and-run: role in exocytosis, endocytosis, and neurotransmission. *Annu. Rev. Physiol.* **2013**, *75*, 393−422.

(17) Peeters, M. C.; van Westen, G. J. P.; Li, Q.; IJzerman, A. P. Importance of the extracellular loops in G protein-coupled receptors for ligand recognition and receptor activation. *Trends Pharmacol. Sci.* **2011**, *32* (1), 35−42.

(18) Schanda, P.; Ernst, M. Studying Dynamics by Magic-Angle Spinning Solid-State NMR Spectroscopy: Principles and Applications to Biomolecules. *Prog. Nucl. Magn. Reson. Spectrosc.* **2016**, *96*, 1−46.

(19) Morris, G. A.; Freeman, R. Enhancement of Nuclear Magnetic-Resonance Signals by Polarization Transfer. *J. Am. Chem. Soc.* **1979**, *101* (3), 760−2.

(20) Gopinath, T.; Nelson, S. E. D.; Soller, K. J.; Veglia, G. Probing the Conformationally Excited States of Membrane Proteins via (1)H-Detected MAS Solid-State NMR Spectroscopy. *J. Phys. Chem. B* **2017**, *121* (17), 4456−65.

(21) Reddy, U. V.; Weber, D. K.; Wang, S.; Larsen, E. K.; Gopinath, T.; De Simone, A.; Robia, S.; Veglia, G. A kink in DWORF helical structure controls the activation of the sarcoplasmic reticulum Ca2+-ATPase. *Structure* **2022**, *30* (3), 360−370.e6.

(22) Weber, D. K.; Reddy, U. V.; Wang, S.; Larsen, E. K.; Gopinath, T.; Gustavsson, M. B.; Cornea, R. L.; Thomas, D. D.; De Simone, A.; Veglia, G. Structural basis for allosteric control of the SERCA-Phospholamban membrane complex by Ca^{2+} and phosphorylation. *eLife* **2021**, *10*, No. e66226, DOI: 10.7554/eLife.66226.

(23) Fusco, G.; Pape, T.; Stephens, A. D.; Mahou, P.; Costa, A. R.; Kaminski, C. F.; Schierle, G. S. K.; Vendruscolo, M.; Veglia, G.; Dobson, C. M.; De Simone, A. Structural basis of synaptic vesicle assembly promoted by α-synuclein. *Nat. Commun.* **2016**, *7*, 12563.

(24) Gopinath, T.; Nelson, S. E. D.; Veglia, G. (1)H-detected MAS solid-state NMR experiments enable the simultaneous mapping of rigid and dynamic domains of membrane proteins. *J. Magn. Reson.* **2017**, *285*, 101−7.

(25) Mansueto, S.; Fusco, G.; De Simone, A. alpha-Synuclein and biological membranes: the danger of loving too much. *Chem. Commun. (Camb)* **2023**, *59* (57), 8769−78.

(26) Chen, S. W.; Barritt, J. D.; Cascella, R.; Bigi, A.; Cecchi, C.; Banchelli, M.; Gallo, A.; Jarvis, J. A.; Chiti, F.; Dobson, C. M.; et al.

Structure-Toxicity Relationship in Intermediate Fibrils from alpha-Synuclein Condensates. *J. Am. Chem. Soc.* **2024**, *146* (15), 10537−49.
(27) Huang, J.; Ahmed, R.; Akimoto, M.; Martinez Pomier, K.; Melacini, G. Early-Onset Parkinson Mutation Remodels Monomer-Fibril Interactions to Allosterically Amplify Synuclein's Amyloid Cascade. *JACS Au* **2023**, *3* (12), 3485−93.
(28) Ahmed, R.; Huang, J.; Weber, D. K.; Gopinath, T.; Veglia, G.; Akimoto, M.; Khondker, A.; Rheinstädter, M. C.; Huynh, V.; Wylie, R. G.; et al. Molecular Mechanism for the Suppression of Alpha Synuclein Membrane Toxicity by an Unconventional Extracellular Chaperone. *J. Am. Chem. Soc.* **2020**, *142* (21), 9686−99.
(29) Lashuel, H. A.; Overk, C. R.; Oueslati, A.; Masliah, E. The many faces of alpha-synuclein: from structure and toxicity to therapeutic target. *Nat. Rev. Neurosci* **2013**, *14* (1), 38−48.
(30) Newberry, R. W.; Leong, J. T.; Chow, E. D.; Kampmann, M.; DeGrado, W. F. Deep mutational scanning reveals the structural basis for alpha-synuclein activity. *Nat. Chem. Biol.* **2020**, *16* (6), 653−9.
(31) Spillantini, M. G.; Schmidt, M. L.; Lee, V. M.; Trojanowski, J. Q.; Jakes, R.; Goedert, M. Alpha-synuclein in Lewy bodies. *Nature* **1997**, *388* (6645), 839−40.
(32) Luk, K. C.; Kehm, V.; Carroll, J.; Zhang, B.; O'Brien, P.; Trojanowski, J. Q.; Lee, V. M. Pathological alpha-synuclein transmission initiates Parkinson-like neurodegeneration in nontransgenic mice. *Science* **2012**, *338* (6109), 949−53.
(33) Chiti, F.; Dobson, C. M. Protein Misfolding, Amyloid Formation, and Human Disease: A Summary of Progress Over the Last Decade. *Annu. Rev. Biochem.* **2017**, *86*, 27−68.
(34) Uversky, V. N.; Eliezer, D. Biophysics of Parkinson's disease: structure and aggregation of alpha-synuclein. *Curr. Protein Pept Sci.* **2009**, *10* (5), 483−99.
(35) Lee, S. J.; Masliah, E. Neurodegeneration: Aggregates feel the strain. *Nature* **2015**, *522* (7556), 296−7.
(36) Kamp, F.; Exner, N.; Lutz, A. K.; Wender, N.; Hegermann, J.; Brunner, B.; Nuscher, B.; Bartels, T.; Giese, A.; Beyer, K.; et al. Inhibition of mitochondrial fusion by alpha-synuclein is rescued by PINK1, Parkin and DJ-1. *EMBO J.* **2010**, *29* (20), 3571−89.
(37) Robotta, M.; Gerding, H. R.; Vogel, A.; Hauser, K.; Schildknecht, S.; Karreman, C.; Leist, M.; Subramaniam, V.; Drescher, M. Alpha-synuclein binds to the inner membrane of mitochondria in an alpha-helical conformation. *Chembiochem* **2014**, *15* (17), 2499−502.
(38) Zigoneanu, I. G.; Yang, Y. J.; Krois, A. S.; Haque, E.; Pielak, G. J. Interaction of alpha-synuclein with vesicles that mimic mitochondrial membranes. *Biochim. Biophys. Acta* **2012**, *1818* (3), 512−9.
(39) Devi, L.; Raghavendran, V.; Prabhu, B. M.; Avadhani, N. G.; Anandatheerthavarada, H. K. Mitochondrial import and accumulation of alpha-synuclein impair complex I in human dopaminergic neuronal cultures and Parkinson disease brain. *J. Biol. Chem.* **2008**, *283* (14), 9089−100.
(40) Nakamura, K.; Nemani, V. M.; Wallender, E. K.; Kaehlcke, K.; Ott, M.; Edwards, R. H. Optical reporters for the conformation of alpha-synuclein reveal a specific interaction with mitochondria. *J. Neurosci.* **2008**, *28* (47), 12305−17.
(41) Guardia-Laguarta, C.; Area-Gomez, E.; Rub, C.; Liu, Y.; Magrane, J.; Becker, D.; Voos, W.; Schon, E. A.; Przedborski, S. alpha-Synuclein is localized to mitochondria-associated ER membranes. *J. Neurosci.* **2014**, *34* (1), 249−59.
(42) Nguyen, M.; Wong, Y. C.; Ysselstein, D.; Severino, A.; Krainc, D. Synaptic, Mitochondrial, and Lysosomal Dysfunction in Parkinson's Disease. *Trends Neurosci* **2019**, *42* (2), 140−9.
(43) Cenini, G.; Lloret, A.; Cascella, R. Oxidative Stress in Neurodegenerative Diseases: From a Mitochondrial Point of View. *Oxid. Med. Cell. Longevity* **2019**, *2019*, 2105607.
(44) Lin, M. T.; Beal, M. F. Mitochondrial dysfunction and oxidative stress in neurodegenerative diseases. *Nature* **2006**, *443* (7113), 787−95.
(45) Nakamura, K.; Nemani, V. M.; Azarbal, F.; Skibinski, G.; Levy, J. M.; Egami, K.; Munishkina, L.; Zhang, J.; Gardner, B.; Wakabayashi, J.; et al. Direct membrane association drives mitochondrial fission by the Parkinson disease-associated protein alpha-synuclein. *J. Biol. Chem.* **2011**, *286* (23), 20710−26.
(46) Butler, E. K.; Voigt, A.; Lutz, A. K.; Toegel, J. P.; Gerhardt, E.; Karsten, P.; Falkenburger, B.; Reinartz, A.; Winklhofer, K. F.; Schulz, J. B. The mitochondrial chaperone protein TRAP1 mitigates alpha-Synuclein toxicity. *PLoS Genet* **2012**, *8* (2), No. e1002488.
(47) Pozo Devoto, V. M.; Falzone, T. L. Mitochondrial dynamics in Parkinson's disease: a role for alpha-synuclein? *Dis Model Mech* **2017**, *10* (9), 1075−87.
(48) Snead, D.; Eliezer, D. Alpha-synuclein function and dysfunction on cellular membranes. *Exp Neurobiol* **2014**, *23* (4), 292−313.
(49) Fusco, G.; Sanz-Hernandez, M.; De Simone, A. Order and disorder in the physiological membrane binding of alpha-synuclein. *Curr. Opin Struct Biol.* **2018**, *48*, 49−57.
(50) Maltsev, A. S.; Ying, J.; Bax, A. Impact of N-terminal acetylation of alpha-synuclein on its random coil and lipid binding properties. *Biochemistry* **2012**, *51* (25), 5004−13.
(51) Bodner, C. R.; Dobson, C. M.; Bax, A. Multiple tight phospholipid-binding modes of alpha-synuclein revealed by solution NMR spectroscopy. *J. Mol. Biol.* **2009**, *390* (4), 775−90.
(52) Ulmer, T. S.; Bax, A.; Cole, N. B.; Nussbaum, R. L. Structure and dynamics of micelle-bound human alpha-synuclein. *J. Biol. Chem.* **2005**, *280* (10), 9595−603.
(53) Eliezer, D.; Kutluay, E.; Bussell, R., Jr.; Browne, G. Conformational properties of alpha-synuclein in its free and lipid-associated states. *J. Mol. Biol.* **2001**, *307* (4), 1061−73.
(54) Fusco, G.; De Simone, A.; Gopinath, T.; Vostrikov, V.; Vendruscolo, M.; Dobson, C. M.; Veglia, G. Direct observation of the three regions in alpha-synuclein that determine its membrane-bound behaviour. *Nat. Commun.* **2014**, *5*, 3827.
(55) Fusco, G.; De Simone, A.; Arosio, P.; Vendruscolo, M.; Veglia, G.; Dobson, C. M. Structural Ensembles of Membrane-bound α-Synuclein Reveal the Molecular Determinants of Synaptic Vesicle Affinity. *Sci. Rep.* **2016**, *6*, 27125.
(56) Navarro-Paya, C.; Sanz-Hernandez, M.; De Simone, A. Plasticity of Membrane Binding by the Central Region of alpha-Synuclein. *Front Mol. Biosci* **2022**, *9*, No. 857217.
(57) Vicario, M.; Cieri, D.; Brini, M.; Calì, T. The Close Encounter Between Alpha-Synuclein and Mitochondria. *Front. Neurosci.* **2018**, *12*, 388.
(58) Parihar, M. S.; Parihar, A.; Fujita, M.; Hashimoto, M.; Ghafourifar, P. Mitochondrial association of alpha-synuclein causes oxidative stress. *Cell. Mol. Life Sci.* **2008**, *65* (7−8), 1272−84.
(59) Man, W. K.; De Simone, A.; Barritt, J. D.; Vendruscolo, M.; Dobson, C. M.; Fusco, G. A Role of Cholesterol in Modulating the Binding of α-Synuclein to Synaptic-Like Vesicles. *Front. Neurosci.* **2020**, *14*, 18.
(60) Man, W. K.; Tahirbegi, B.; Vrettas, M. D.; Preet, S.; Ying, L.; Vendruscolo, M.; De Simone, A.; Fusco, G. The docking of synaptic vesicles on the presynaptic membrane induced by α-synuclein is modulated by lipid composition. *Nat. Commun.* **2021**, *12* (1), 927.
(61) Zhou, D. H.; Rienstra, C. M. High-performance solvent suppression for proton detected solid-state NMR. *J. Magn. Reson.* **2008**, *192* (1), 167−72.
(62) Adamski, W.; Salvi, N.; Maurin, D.; Magnat, J.; Milles, S.; Jensen, M. R.; Abyzov, A.; Moreau, C. J.; Blackledge, M. A Unified Description of Intrinsically Disordered Protein Dynamics under Physiological Conditions Using NMR Spectroscopy. *J. Am. Chem. Soc.* **2019**, *141* (44), 17817−29.
(63) Lu, Y.; Prudent, M.; Fauvet, B.; Lashuel, H. A.; Girault, H. H. Phosphorylation of alpha-Synuclein at Y125 and S129 alters its metal binding properties: implications for understanding the role of alpha-Synuclein in the pathogenesis of Parkinson's Disease and related disorders. *ACS Chem. Neurosci.* **2011**, *2* (11), 667−75.
(64) Lautenschläger, J.; Stephens, A. D.; Fusco, G.; Strohl, F.; Curry, N.; Zacharopoulou, M.; Michel, C. H.; Laine, R.; Nespovitaya, N.; Fantham, M.; et al. C-terminal calcium binding of α-synuclein modulates synaptic vesicle interaction. *Nat. Commun.* **2018**, *9* (1), 712.

https://doi.org/10.1021/jacsau.4c00323
JACS Au XXXX, XXX, XXX−XXX

(65) Kjaergaard, M.; Kragelund, B. B. Functions of intrinsic disorder in transmembrane proteins. *Cell. Mol. Life Sci.* **2017**, *74* (17), 3205−24.
(66) Araya, M. K.; Zhou, Y.; Gorfe, A. A. Remodeling of the Plasma Membrane by Surface-Bound Protein Monomers and Oligomers: The Critical Role of Intrinsically Disordered Regions. *J. Membr. Biol.* **2022**, *255* (6), 651−63.
(67) Zeno, W. F.; Baul, U.; Snead, W. T.; DeGroot, A. C. M.; Wang, L.; Lafer, E. M.; Thirumalai, D.; Stachowiak, J. C. Synergy between intrinsically disordered domains and structured proteins amplifies membrane curvature sensing. *Nat. Commun.* **2018**, *9* (1), 4152.
(68) Mikros, E.; Diallinas, G. Tales of tails in transporters. *Open Biol.* **2019**, *9* (6), No. 190083.
(69) Dyson, H. J.; Wright, P. E. Insights into the structure and dynamics of unfolded proteins from nuclear magnetic resonance. *Adv. Protein Chem.* **2002**, *62*, 311−340.
(70) Theillet, F. X.; Binolfi, A.; Bekei, B.; Martorana, A.; Rose, H. M.; Stuiver, M.; Verzini, S.; Lorenz, D.; van Rossum, M.; Goldfarb, D.; Selenko, P. Structural disorder of monomeric alpha-synuclein persists in mammalian cells. *Nature* **2016**, *530* (7588), 45−50.
(71) Im, J.; Lee, J.; Lee, J. H. Surface Accessibility of an Intrinsically Disordered Protein Probed by 2D Time-Resolved Laser-Assisted NMR Spectroscopy. *J. Am. Chem. Soc.* **2022**, *144* (37), 17010−21.
(72) Danmaliki, G. I.; Hwang, P. M. Solution NMR spectroscopy of membrane proteins. *Biochim Biophys Acta Biomembr* **2020**, *1862* (9), No. 183356.
(73) Mandala, V. S.; Williams, J. K.; Hong, M. Structure and Dynamics of Membrane Proteins from Solid-State NMR. *Annu. Rev. Biophys* **2018**, *47*, 201−22.
(74) Gopinath, T.; Weber, D.; Wang, S.; Larsen, E.; Veglia, G. Solid-State NMR of Membrane Proteins in Lipid Bilayers: To Spin or Not To Spin? *Acc. Chem. Res.* **2021**, *54* (6), 1430−9.
(75) Briggs, E. L. A.; Gomes, R. G. B.; Elhussein, M.; Collier, W.; Findlow, I. S.; Khalid, S.; McCormick, C. J.; Williamson, P. T. F. Interaction between the NS4B amphipathic helix, AH2, and charged lipid headgroups alters membrane morphology and AH2 oligomeric state — Implications for the Hepatitis C virus life cycle. *Biochim. Biophys. Acta Biomembr.* **2015**, *1848* (8), 1671−1677.
(76) Gallo, A.; Franks, W. T.; Lewandowski, J. R. A suite of solid-state NMR experiments to utilize orphaned magnetization for assignment of proteins using parallel high and low gamma detection. *J. Magn. Reson.* **2019**, *305*, 219−231.
(77) Barbet-Massin, E.; Pell, A. J.; Knight, M. J.; Webber, A. L.; Felli, I. C.; Pierattelli, R.; Emsley, L.; Lesage, A.; Pintacuda, G. 13C-detected through-bond correlation experiments for protein resonance assignment by ultra-fast MAS solid-state NMR. *ChemPhysChem* **2013**, *14* (13), 3131−7.
(78) Schubeis, T.; Stanek, J.; Pintacuda, G. Backbone assignment of crystalline E. coli maltose binding protein. *Biomol NMR Assign* **2021**, *15* (2), 317−22.
(79) Andreas, L. B.; Le Marchand, T.; Jaudzems, K.; Pintacuda, G. High-resolution proton-detected NMR of proteins at very fast MAS. *J. Magn. Reson.* **2015**, *253*, 36−49.
(80) Stanek, J.; Andreas, L. B.; Jaudzems, K.; Cala, D.; Lalli, D.; Bertarello, A.; Schubeis, T.; Akopjana, I.; Kotelovica, S.; Tars, K.; et al. NMR Spectroscopic Assignment of Backbone and Side-Chain Protons in Fully Protonated Proteins: Microcrystals, Sedimented Assemblies, and Amyloid Fibrils. *Angew. Chem., Int. Ed. Engl.* **2016**, *55* (50), 15504−9.
(81) Dedmon, M. M.; Lindorff-Larsen, K.; Christodoulou, J.; Vendruscolo, M.; Dobson, C. M. Mapping long-range interactions in alpha-synuclein using spin-label NMR and ensemble molecular dynamics simulations. *J. Am. Chem. Soc.* **2005**, *127* (2), 476−7.
(82) Burre, J.; Sharma, M.; Tsetsenis, T.; Buchman, V.; Etherton, M. R.; Sudhof, T. C. Alpha-synuclein promotes SNARE-complex assembly in vivo and in vitro. *Science* **2010**, *329* (5999), 1663−7.
(83) Ryan, T.; Bamm, V. V.; Stykel, M. G.; Coackley, C. L.; Humphries, K. M.; Jamieson-Williams, R.; Ambasudhan, R.; Mosser, D. D.; Lipton, S. A.; Harauz, G.; Ryan, S. D. Cardiolipin exposure on the outer mitochondrial membrane modulates α-synuclein. *Nat. Commun.* **2018**, *9* (1), 817.
(84) Farrow, N. A.; Muhandiram, R.; Singer, A. U.; Pascal, S. M.; Kay, C. M.; Gish, G.; Shoelson, S. E.; Pawson, T.; Forman-Kay, J. D.; Kay, L. E. Backbone dynamics of a free and phosphopeptide-complexed Src homology 2 domain studied by 15N NMR relaxation. *Biochemistry* **1994**, *33* (19), 5984−6003.
(85) Piotto, M.; Saudek, V.; Sklenar, V. Gradient-tailored excitation for single-quantum NMR spectroscopy of aqueous solutions. *J. Biomol NMR* **1992**, *2* (6), 661−5.
(86) Fusco, G.; Sanz-Hernandez, M.; Ruggeri, F. S.; Vendruscolo, M.; Dobson, C. M.; De Simone, A. Molecular determinants of the interaction of EGCG with ordered and disordered proteins. *Biopolymers* **2018**, *109* (10), e23117.
(87) Fusco, G.; De Simone, A.; Hsu, S. T.; Bemporad, F.; Vendruscolo, M.; Chiti, F.; Dobson, C. M. (1)H, (1)(3)C and (1)(5)N resonance assignments of human muscle acylphosphatase. *Biomol NMR Assign* **2012**, *6* (1), 27−9.

https://doi.org/10.1021/jacsau.4c00323
JACS Au XXXX, XXX, XXX−XXX